Sub-Optimum Design of a Forced Air Cooled Heat Sink for Simple Manufacturing

Uwe DROFENIK and Johann W. KOLAR

Power Electronic Systems Laboratory, ETH Zurich, ETH-Zentrum / ETL H13, CH-8092 Zurich, Switzerland
Phone: +41-1-632-4267, Fax: +41-1-632-1212, E-mail: **drofenik@lem.ee.ethz.ch**

Abstract — **In order to maximize the power density of a converter, a systematic procedure for optimizing the cooling system is necessary. Solving the equations of the optimization procedure described in this paper can be performed numerically without much effort, but manufacturing the resulting optimum heat sink is often extremely difficult and expensive, and therefore impractical. Based on the optimization theory, the sensitivity of the thermal resistance of the heat sink to changes in the geometric design parameters is discussed. Diagrams show the expected increase in thermal resistance if the manufacturing process constrains the fin thickness to certain values. Based on this, one can design a sub-optimum heat sink that gives the minimum thermal resistance for a certain manufacturing procedure. Furthermore, it is shown how much additional manufacturing effort would be necessary to further improve the performance of the heat sink. The proposed procedure is verified experimentally.**

Index Terms — **design parameter sensitivity, heat sink optimization, high power density**

I. INTRODUCTION

Finding the optimum heat sink geometry for a certain fan could be done by numerical 3D-simulations of the heat transfer for different geometric parameter sets, but this is of very high computational effort. At least two geometric heat sink parameters (e.g., fin number and fin thickness) have to be varied, which results in a large number of time-consuming simulations, in order to systematically find an optimum design (with minimum thermal resistance). Considering different fans will further increase the parameter space.

In section II we propose an optimization strategy based on analytical and empirical equations that describe conductive heat transfer through fins and convective heat transfer in the air channels of the heat sink. The resulting equation set, which is dependent on heat sink parameters and fan characteristic, is easy to solve and immediately gives the optimum heat sink geometry for a given fan.

Finding the optimum heat sink geometry, which gives minimum thermal resistance for a given fan and a given base plate size to attach all power semiconductors, often results in very thin fins and/or very small channel widths, which is sometimes very hard or even impossible to manufacture. It is, therefore, of high practical interest, how much changes of the theoretical optimum geometry will reduce the heat sink performance.

In section III, the sensitivity of the geometric heat sink parameters concerning the thermal resistance is calculated and shown graphically. Based on such diagrams, a designer can quickly find out how much the thermal resistance is increased if fin thickness and/or channel width are restricted by manufacturing constraints. Sub-optimum designs can be identified which give the minimum thermal resistance for the available manufacturing technology.

In section IV the proposed procedure is applied to the design of the cooling system for a 5kW high power density DC/DC converter. The sub-optimum design is compared to the theoretical optimum, and measurements of prototypes are given.
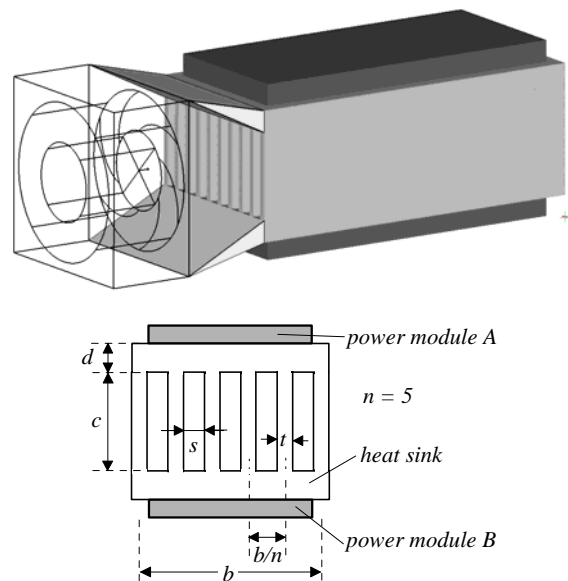

Fig.1. A square-shaped fan ($b \times b$) faces a rectangular-shaped heat sink ($b \times c$, $b > c$) with power module A on top and, symmetrically, power module B on bottom. The air flow is guided by two triangular-shaped structures in order to minimize the air pressure drop before the air-flow is entering the heat sink channels. The according heat transfer is described by equations (11) – (14).

II. GENERAL OPTIMIZATION PROCEDURE OF A FORCED AIR COOLING SYSTEM

The heat sink to be optimized for a 5kW DC/DC converter is shown in **Fig.1**. The optimization procedure (1) – (10) is described in detail in [1] and [2]. Based on (1) – (5) one can calculate the air flow pressure drop in the heat sink channels for laminar and turbulent flow.

Balancing the pressure drop with the pressure of the fan Δp_{FAN} as defined by the fan characteristic in (6) gives the fan operating point, defining flow and pressure drop in the heat sink channels. If the resulting Reynolds number is smaller than *2300*, the flow is considered to be laminar, and (7) has to be employed to get the Nusselt number, which describes the convective heat transfer from channel wall into the air. In case of turbulent flow ($Re_m>2300$), the Nusselt number is calculated from (9). Employing (10), the heat transfer coefficient of the configuration is found. The geometric parameters employed in (1) – (10) are shown in **Fig.2**.

k	fin spacing ratio
λ_{HS} [W/mK]	thermal conductivity of heat sink material
A_{HS} [m²]	size of the heat sink base plate
d_h [m]	hydraulic diameter of one channel
L [m]	channel length in air flow direction
n	number of channels
Δp [N/m²]	pressure drop in one channel
V [m³/s]	volume flow
Re_m	avg. Reynolds number (for lam. or turb. flow)
Nu_m	avg. Nusselt number (for lam. or turb. flow)
h [W/m²K]	(convective) heat transfer coefficient
$Pr \approx 0.71$	Prandtl number (air, 80°C)
$\rho_{AIR} \approx 0.99$ [kg/m³]	air density (80°C)
$v_{AIR} \approx$ 2.1e-5 [m²/s]	cinematic viscosity of the air (80°C)
$c_{p,AIR} \approx 1010$ [J/kgK]	specific thermal capacitance of air
$\lambda_{AIR} \approx 0.03$ [W/mK]	thermal conductivity of air (80°C)

$$k = \frac{s}{b/n} \tag{1}$$

$$d_h = \frac{2s \cdot c}{s + c} \tag{2}$$

$$\Delta p_{lam}(V) = \frac{48 \, \rho_{AIR} \, v_{AIR} \, L}{n \, (s \cdot c) \, d_h^2} \, V \tag{3}$$

$$\Delta p_{turb}(V) = \frac{L \frac{s+c}{2s \cdot c} \rho_{AIR} \frac{1}{2} \left(\frac{V}{n(s \cdot c)}\right)^2}{\left(0.79 \cdot \ln\left(\frac{2V}{n \, (s+c) v_{AIR}}\right) - 1.64\right)^2} \tag{4}$$

$$Re_m = \frac{2V}{n(s+c) v_{AIR}} \tag{5}$$

$$k \cdot \Delta p_{FAN}(V) = \Delta p_{lam}(V_{lam}) \rightarrow V_{lam} \rightarrow Re_{m,lam} < 2300 \,? \tag{6}$$

$$Nu_{m,lam} = \frac{3.657\left[\tanh\left(2.264X^{1/3} + 1.7X^{2/3}\right)\right]^{-1} + \frac{0.0499}{X} \tanh(X)}{\tanh\left[2.432 \, Pr^{1/6} X^{1/6}\right]} \tag{7}$$

$$X = \frac{L}{d_h \, Re_m \, Pr} \tag{8}$$

$$Nu_{m,turb} = \frac{\{8 \cdot (0.79 \cdot \ln(Re_m) - 1.64)^2)\}^{-1} (Re_m - 1000) \, Pr}{1 + 12.7 \sqrt{\{8 \cdot (0.79 \cdot \ln(Re_m) - 1.64)^2)\}^{-1} (Pr^{2/3} - 1)}} \cdot$$
$$\cdot \left(1 + \left(\frac{d_h}{L}\right)^{2/3}\right) \tag{9}$$

$$h = \frac{Nu_m \cdot \lambda_{AIR}}{d_h} \tag{10}$$

For the design as shown in Fig.1 with one power module A on the top and a second module B with approximately equal losses attached to the bottom side, the conductive heat transfer through the fins is modeled according to Fig.2. Equations (11) – (14) give the thermal resistance of this heat sink as experienced by one of the two power modules (A and/or B). The last term of the thermal resistance in (14) considers the average temperature rise of the air from channel inlet to channel outlet.
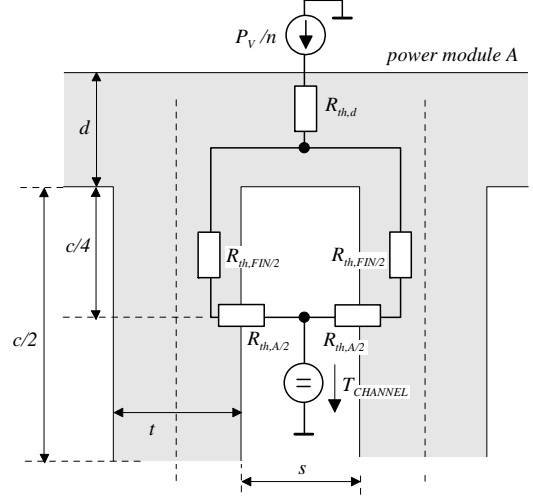

Fig.2. Thermal equivalent circuit of the heat flow from power module A into the air flowing through the channel. Only the upper half of the symmetrical heat sink structure is shown.

$$R_{th,A/2} = \frac{1}{h \cdot L \cdot \frac{1}{2}c} \tag{11}$$

$$R_{th,FIN/2} = \frac{\frac{1}{4}c}{\frac{1}{2}t \cdot L \cdot \lambda_{HS}} \tag{12}$$

$$R_{th,d} = \frac{d}{\frac{1}{n} A_{HS} \lambda_{HS}} \tag{13}$$

$$R_{th,S-a}^{(HS)} = \frac{1}{n}(R_{th,d} + \frac{1}{2}(R_{th,FIN/2} + R_{th,A/2})) + \frac{0.5}{\rho_{AIR} \, c_{P,AIR} \cdot \frac{1}{2}V} \tag{14}$$

III. SENSITIVITY OF THE OPTIMUM DESIGN CONCERNING CHANGES IN THE GEOMETRIC PARAMETERS

In this section, the proposed optimization procedure is tested and extended for heat sinks that are slightly different from the one shown in Fig.1, employing just one single power module mounted onto the top base plate as shown in **Fig.3**. This also demonstrates the flexibility of the approach in case of minor changes of the basic heat sink configuration. The optimization procedure for the air flow described by (1) – (10) is still valid, but the heat transfer through the fins has to be adapted by employing (15) – (17) instead of (11) – (14).
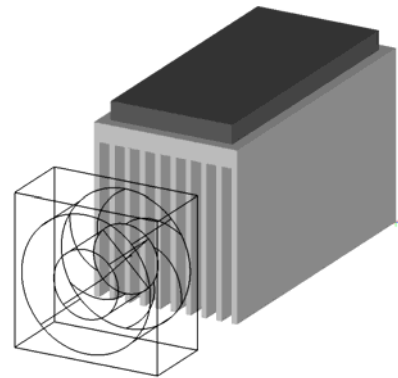

Fig.3. Heat sink with a single power module with fin height c, fin thickness t, channel width s, base plate thickness d and heat sink length L. The according heat transfer is described by equations (15) – (17).

$$R_{th,A} = \frac{1}{h \cdot L \cdot c} \tag{15}$$

$$R_{th,FIN} = \frac{\frac{1}{2}c}{\frac{1}{2}t \cdot L \cdot \lambda_{HS}} \tag{16}$$

$$R_{th,S-a}^{(HS)} = \frac{1}{n}\left(R_{th,d} + \frac{1}{2}(R_{th,FIN} + R_{th,A})\right) + \frac{0.5}{\rho_{AIR}\, c_{P,AIR} \cdot V} \tag{17}$$

Solving (1) – (11) and (15) – (17) numerically for different parameters which characterize the heat sink geometry, gives the diagram shown in **Fig.4** for aluminum and, alternatively, copper as heat sink materials. In Fig.4 we assumed a minimum chip area $A_{CHIP,MIN} = 32cm^2$ and a heat sink maximum height of $c = 40mm$. The selected fan is a SanAce40/50dB [3] for server-applications which is one of the strongest fans commercially available in this application area. The two geometric parameters that can be varied independently are the number of fins n and the fin spacing ration k defined in equation (1).
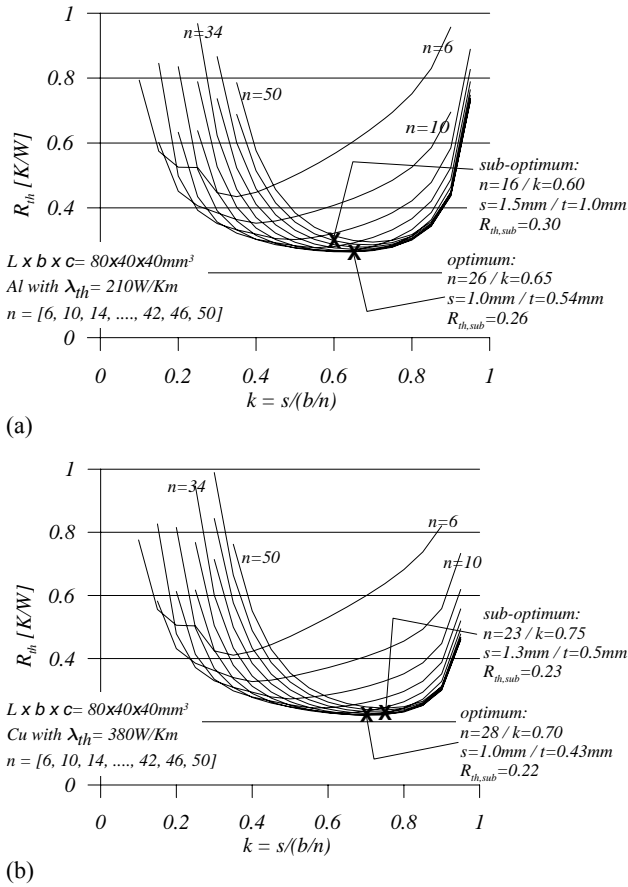

(a)

(b)

Fig.4. Sensitivity of the thermal resistance for a variation of geometric heat sink parameters for a heat sink design according to Fig.3. The heat sink material is (a) aluminum (210W/Km), (b) copper (380W/Km). The dimensions are $L=80mm$, $b=40mm$, $c=40mm$, $d=10mm$. As fan we employed SanAce40/50dB.

The theoretical optimum design for aluminum shows 26 fins with fin thickness *0.54mm* and channel width *1.0mm* resulting in a thermal resistance of *0.26K/W*. This is difficult to manufacture, especially due to the fin height of *40mm*. Since the optimum is located at a very flat section of the curves, one can select a sub-optimum

which is easier to manufacture, but still providing a thermal resistance close to the theoretical minimum. In Fig.4 a possible sub-optimum is selected at fin number *n=16*, fin thickness *1.0mm*, and channel spacing *1.5mm*. The thermal resistance of the sub-optimum is *0.30K/W* which is a performance reduction of just *15%*, although the fin number is reduced by *38%*, the fin thickness is increased by *85%*, and the channel width is increased by *50%*.

Although the thermal conductivity of copper ($\lambda_{Cu}=380W/Km$) is nearly twice the conductivity of aluminum ($\lambda_{Al}=210W/Km$), the optimum thermal resistance of the copper heat sink $R_{th,MIN,Cu}=0.22K/W$ is just *15%* smaller than for the aluminum heat sink. This is due to the strongly nonlinear relationship between air flow, pressure drop, and convective heat transfer as described in (1) – (10). In case of different configurations, such as shorter heat sinks ($L<80mm$), the potential improvement of copper employment might be significant for certain designs. In this design example, the improvement is quite small, but the heat sink is nearly four times heavier.

Manufacturing a heat sink prototype with a sub-optimum geometry as described in Fig.4 is extremely difficult and not reliable if one tries to cut slots with a saw into a block of aluminum or copper. Alternatively, spark erosion could be used to produce a prototype but this is extremely expensive and very time-consuming. Therefore, we employed a procedure where pre-manufactured metal plates of defined thickness are stacked, pressed together and fixed by screws as shown schematically in **Fig.5**. The heat spreading capability of the heat sink base plate is reduced, but if the attached power module provides an internal heat spreader and covers most of the heat sink base plate area, the effect will be neglectable. In this case the main heat flow will be in-plane through each stacked fin plate. Therefore, the procedure will give good results even in case of using thermal materials with anisotropic (in-plane) thermal conductivity like Highly Orientated Pyrolytic Graphite (HOPG) [2].
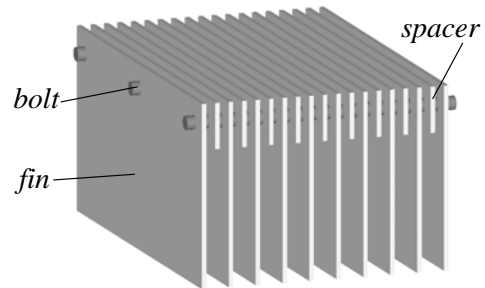

Fig.5. Construction of a stacked heat sink. Fin and spacer are metal plates with defined thickness.

For manufacturing, the following plate thicknesses were available from a local supplier: Aluminum-plates of *210W/Km* with *0.3mm*, *0.5mm*, *0.8mm*, *1.0mm*, and *1.5mm*, and copper-plates of *380W/Km* with *0.5mm*,

0.6mm, 0.7mm, 0.8mm, 0.9mm, 1.0mm, 1.2mm, 1.3mm and *1.5mm*. For all following design examples (also section IV) the sub-optima are selected based on these available thicknesses. The assembled heat sinks of the sub-optimum designs defined in Fig.4 are shown in **Fig.6**.

The measurement of the thermal resistance of the heat sink was performed by replacing the power module by a heat source made by a thick copper plate with heating resistors placed on top (see section IV and [4] for details). This heat source has to be thermally isolated so that ideally all heat flows directly from the heating resistors through the copper block into the heat sink base plate. The copper block acts as a heat spreader creating an equally distributed thermal power flow. The temperature inside the copper block is assumed to be in good approximation constant because of its small dimensions (compared to the heat sink) and the high thermal conductivity of copper. The base plate temperature is measured by a K-type thermocouple (accuracy 2%, see [5]) placed inside a hole (*2mm* diameter) drilled into the center of the copper block. The temperature difference between the copper block center temperature and the inlet air temperature is divided by the thermal power (which is approximately equal to the product of voltage and current at the heating resistor) to get the thermal resistance of the heat sink.

(a)   (b)

Fig.6. Sub-optimum stacked heat sinks employing SanAce40/50dB (not shown) with *b=c=40mm, d=10mm, L=80mm, $A_{CHIP}= 32cm^2$, $Vol_{CS}= 0.4\times(0.4+0.1)\times(0.80+0.05+0.28)= 0.226$ liter*. (a) Aluminum with *n=16, s=1.5mm, t=1.0mm, R_{th}=0.26*. (b) Copper with *n=23, s=1.3mm, t=0.5mm, R_{th}=0.22*.

The measured thermal resistances of the heat sinks in Fig.6 verify the theoretical calculations with good accuracy. For aluminum (Fig.6(a)), we measured *R_{th}=0.26 K/W* (theory: *R_{th}=0.30 K/W*), and for copper (Fig.6(b)) we measured *R_{th}=0.22 K/W* (theory: *R_{th}=0.23 K/W*). Compared to an aluminum heat sink produced by spark-erosion out of a homogenous aluminum block with exactly the same dimensions as the sub-optimum heat sink in Fig.6(a), the measured thermal resistance of the stacked version was 5% larger due to the reduced heat spreading through the base plate.

IV APPLYING THE THEORY FOR DESIGNING A COOLING SYSTEM FOR A 5KW DC-DC CONVERTER

For a heat sink design, as shown in Fig.6, the fan fully faces the channels and, therefore, the width and height of the heat sink are defined by the fan dimensions as *b=c*. To make the design more flexible, especially if the maximum acceptable height of heat sink plus attached power modules is limited, the airflow from fan to heat sink channels has to be guided with minimum pressure loss as shown in Fig.1. Then, it is possible to set *c<b*. Furthermore, (different from the design in Fig.3 and/or Fig.6) a heat flow is impressed from both sides of the heat sink, which is considered by equations (11) – (14). This is of advantage compared to the design in Fig.3 because there is much better utilization of the fin material for heat conduction.
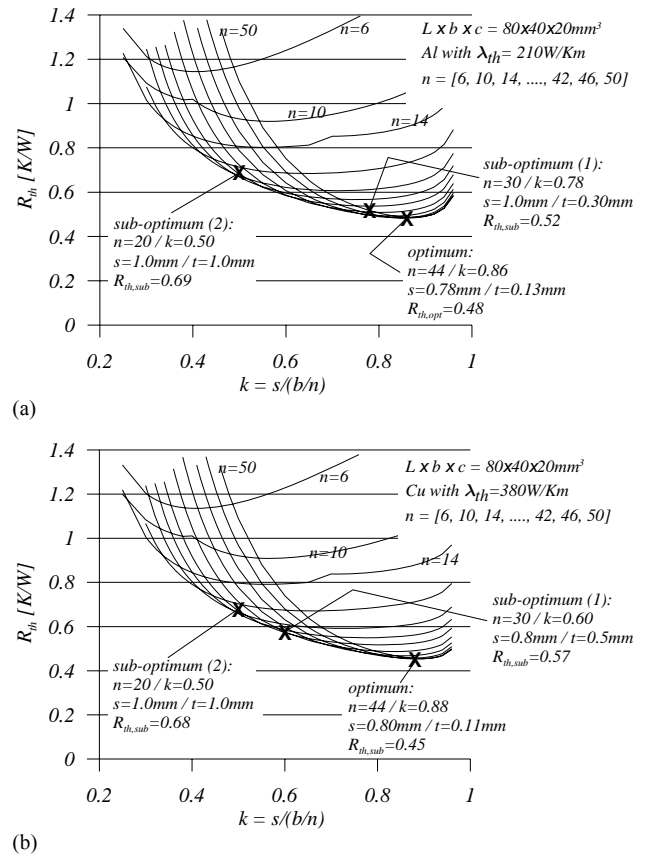

(a)

(b)

Fig.7. Sensitivity of the thermal resistance (as experienced by power module A) for variation of the geometric heat sink parameters for the design shown in Fig.1. The heat sink material is (a) aluminum (*210W/Km*), (b) copper (*380W/Km*). The general dimensions are *L=80mm, b=40mm, c=20mm, d=5mm*. As fan we employed SanAce40/50dB.

For a 5kW-DC/DC converter with certain geometric limitations an optimized heat sink (minimum thermal resistance at minimum volume) has to be designed. Based on the basic design shown in Fig.1, the following geometric parameters are given: *L=80mm, b=40mm, c=20mm, d=5mm*. Employing a comparably strong fan SanAce40/50dB, the thermal resistance based on fin number and fin spacing ration is numerically calculated

via (1) – (14) and shown in **Fig.7** for aluminum and copper.

Sub-optimum points (1) in the parameter space are defined for the available plate thicknesses (as given in section III) for stacked heat sinks. Alternatively, sub-optimum points (2) are given for channel width of *1mm* and fin thickness of *1mm* which is the minimum dimension that could be manufactured without major problems by sawing slots into a metal block of the according dimensions.

As one can see in the two diagrams ((a) aluminum and (b) copper) of Fig.7, the difference in thermal resistance is extremely small for this design although the thermal conductivity of copper is nearly twice as that of aluminum. Only in case of the theoretical optimum, the aluminum heat sink's resistance (*0.48 K/W*) is higher than that of copper (*0.45 K/W*), but in this ideal case the improvement is only about 6% and the copper heat sink is four times heavier than the aluminum heat sink. At sub-optimum design (2), copper and aluminum are approximately equal, and at sub-optimum design (1) aluminum gives better results than copper. This is, of course, only possible because of our manufacturing condition described in section III, which provides aluminum plates as thin as *0.3mm*, while the thinnest available copper plates are *0.5mm*. In case of equal geometry the heat sink employing material of higher thermal conductivity must always show at least slightly lower thermal resistance.

As also described in the previous section, it is very important to understand that the comparison of different materials in Fig.7 provides no general rule but is a result of the very special geometric conditions for our example (the 5kW DC/DC-Converter) and of our special side condition of available metal plate thicknesses. For different design geometries the influence of the heat sink material can be significant, and in many cases the improvement by employing copper instead of aluminum is quite large (see [1] and [2] for further examples and detailed discussions).
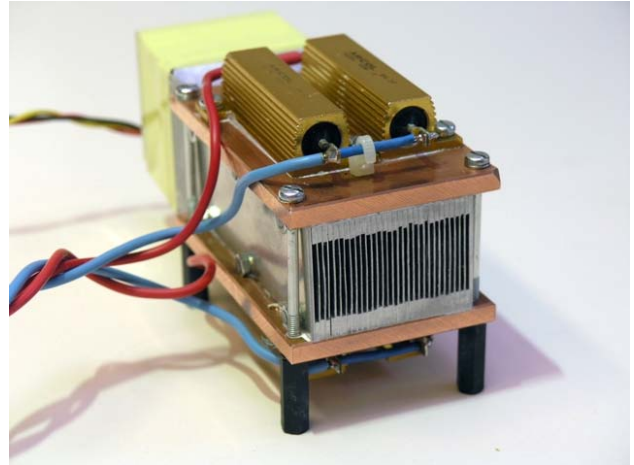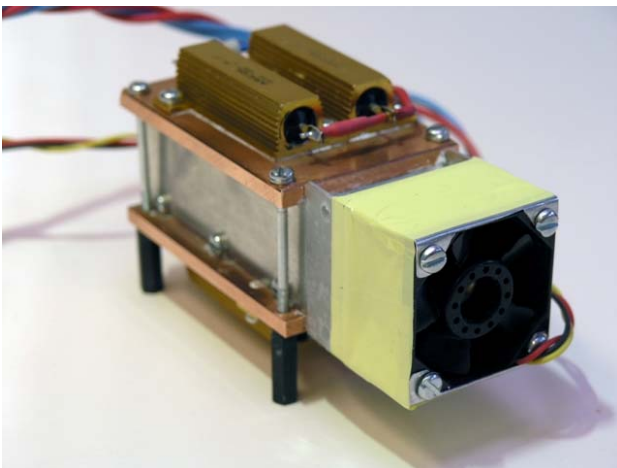

Fig.8. Sub-optimum stacked aluminum heat sink employing SanAce40/50dB with dimensions *L=80mm, b=40mm, c=20mm, d=5mm, A_{CHIP}= 32cm², Vol_{CS}= 0.4×0.4×(0.80+0.28+0.14)= 0.195 liter*. The copper heat spreading plates plus heating resistors as described in section III are mounted onto the heat sink (thermal isolation not shown). Employing aluminum as heat sink material, sub-optimum design (1) gives *n=30, s=1.0mm, t=0.3mm*. Measured thermal resistance as experienced from the top (or bottom) side is *R_{th}=0.56*.

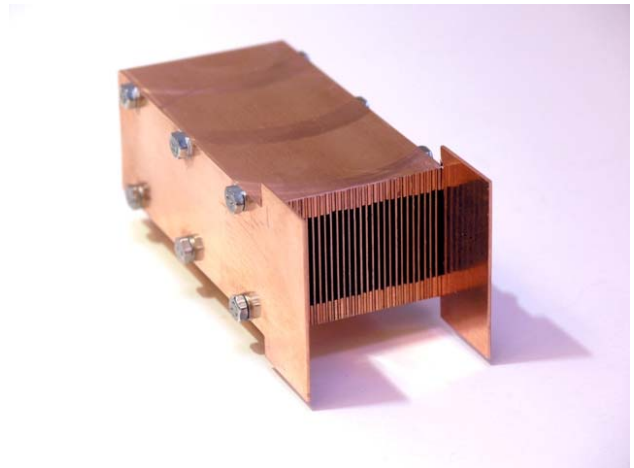Fig.9. Sub-optimum stacked copper heat sink with dimensions *L=80mm, b=40mm, c=20mm, d=5mm, A_{CHIP}= 32cm², Vol_{CS}= 0.4×0.4×(0.80+0.28+0.14) = 0.195 liter*. Employing copper, sub-optimum design (1) gives *n=30, s=0.8mm, t=0.5mm*. Measured thermal resistance as experienced from the top (or bottom) side is *R_{th}=0.68*.

The sub-optimum design (1) of Fig.7 is realized as stacked heat sink (Fig.5) for aluminum (**Fig.8**) and copper (**Fig.9**). In Fig.8, one can see the heating resistors mounted onto copper blocks as described in section III for measuring the thermal resistance of the heat sink. The thermal resistance of one side of the aluminum heat sink (top or bottom) in Fig.8 is measured as R_{th} = *0.56 K/W* which is 7% larger than the theoretical value ($R_{th,SubOpt(1)}$ = *0.52 K/W*). For the copper heat sink in Fig.9, we measured R_{th} = *0.68 K/W* which is 16% larger than the theoretical value ($R_{th,SubOpt(1)}$ = *0.57 K/W*). The two measurements also confirm the result of the theoretical calculations: Although the thermal conductivity of copper is much higher than that of aluminum, the thermal

resistance of the aluminum heat sink is slightly lower than that of the copper heat sink, while the geometric differences (same fin number but different fin thickness) are very small. In the theoretical result shown in Fig.7 the difference of the thermal resistances for the two aluminum and copper is 10%, the measurements of the two prototype heat sinks (Fig.8 and Fig.9) gives a difference of 21%.

With the definition of the *Cooling System Performance Index CSPI* [1] for convenient comparison of different cooling system designs, we get for the aluminum cooling system of Fig.8

$$CSPI\left[\tfrac{W}{K \cdot liter}\right] = \frac{1}{R_{th,S-a}\left[\tfrac{K}{W}\right] \cdot V_{CS}\left[liter\right]} = \frac{1}{\tfrac{1}{2} \cdot 0.56 \cdot 0.195} = \underline{\underline{18.3}}$$

(18)

which is quite high compared to alternative system designs (e.g., compare values in Tab.3 in [1]). In this case, the cooling system volume V_{CS} consists of heat sink ($L=80mm$), fan ($L_F=28mm$) and air flow channel between fan and heat sink of length $L_C=14mm$. Since $R_{th}=0.56$ K/W is experienced from just one base plate of the heat sink, the thermal resistance in (18) has to be divided by two to take both base plates (top and bottom) into account.

V. CONCLUSIONS

Optimizing a heat sink for minimum thermal resistance at minimum volume often results in fin and channel geometries that are very hard or even impossible to manufacture. In order to fulfill manufacturing constraints that are imposed due to available machines, available materials or pre-defined cost targets, one often has to choose a sub-optimum heat sink geometry.

In this paper we propose a mathematical procedure to obtain graphic diagrams, that show how much the thermal resistance of a heat sink will increase compared to the theoretical minimum value, if the fin thickness or number of fins is changed.

The proposed procedure is verified by experimental measurements for four different heat sink designs. The heat sinks have been realized by stacking together fin plates and spacer plates as shown in the paper. This assembly method proofed to be very useful in building heat sink prototypes with extremely thin fins and channels.

REFERENCES

[1] U. Drofenik, G. Laimer, J. W. Kolar, "Theoretical Converter Power Density Limits for Forced Convection Cooling", in *Proceedings of the International PCIM Europe 2005 Conference*, Nuremberg, Germany, June 7 - 9, pp. 608 - 619 (2005).

[2] U. Drofenik, J. W. Kolar, "Analyzing the Theoretical Limits of Forced Air-Cooling by Employing Advanced Composite Materials with Thermal Conductivities > 400W/mK", in *Proceedings of the 4th International Conference on Integrated Power Systems (CIPS'06)*, Naples, Italy, June 7 - 9 (2006).

[3] Sanyo Denki Co., Ltd., http://www.sanyodenki.co.jp/, Webcatalog, Cooling Fan and CPU-Cooler, DC-Fan, datasheets published at http://sanyodb.colle.co.jp/product_db_e/coolingfan/dcfan/dc_fan_detail.php?master_id=1178 (January 2007)

[4] U. Drofenik, G. Laimer, J. W. Kolar, "Pump Characteristic Based Optimization of a Direct Water Cooling System for a 10kW/500kHz Vienna Rectifier" in the *IEEE Transactions on Power Electronics*, vol. 20, no. 3, pp. 704-714, May 2005.

[5] Fluke, http://www.fluke.ch/, "80BK Integrated DMM Temperature Probe," datasheet published at http://www.fluke.ch/comx/show_product.aspx?locale=chde&pid=23290 (January 2007)